International Research Journal of Multidisciplinary Scope (IRJMS), 2025; 6(3):839-850 IRJMS

Original Article | ISSN (O): 2582-631X DOI: 10.47857/irjms.2025.v06i03.04205

Deep Learning-Based Segmentation System for Renal Tumors

Gomalavalli R[1], Veera Boopathy E[2]*, Hema J[3]

[1]Sri Sairam Institute of Technology, Chennai, India, [2]Department of ECE, Karpagam Institute of Technology, Coimbatore, India, [3]Anna University, Chennai, India. *Corresponding Author's Email: boopathy.veera@gmail.com

Abstract

This research set out to conduct a comprehensive analysis of methods currently used for segmenting renal tumors from CT images. Renal tumor (RT) remains maximum prevalent tumor for all globally, and it is one of the diseases that have greatly impacted our culture. In comparison to the time-consuming and labor-intensive method of conventional analysis, the automated recognition procedures of deep learning (DL) shall speed up analysis, tweak test precision, decrease expenses, besides relieve strain on radiologists. Here, detection models proposed which can be used to identify RTs in CT scans. Investigators in the area of medical imaging segmentation utilizes DL techniques for tackling difficulties in tumor delineation, cell delineation, and organ segmentation all at once. For radiation and therapeutic purposes, semantic tumors segmentation is essential. Automated recognition algorithms based on predictive modeling might speed up the diagnostic process, improve test precision, and reduce expenses contrast to lengthy, prolonged traditional methods. The hybrid V-Net method determines the renal segmentation of 0.977 and tumor segmentation of 0.865. A 300CT datasets are utilized to obtain the 91-99% of accuracy in modified CNN and 3 cross folds. Renal tumors are among the deadliest types of tumors, and previous research has demonstrated that deep learning can aid detection, segmentation, and categorization of this disease. Modern developments in DL-based segmentation systems for renal tumors are discussed in this article. Here, the components of renal tumor segmentation outlined, including the numerous medical picture types and segmentation algorithms, as well as the assessment criteria for segmentation outcomes.

Keywords: CNN, Computer Tomography (CT), CT Image Segmentation, Deep Learning, Renal Tumor Segmentation.

Introduction

A radiologist's everyday tasks include the visual examination of various anatomical components within medical imaging. Subtle morphological changes may be diagnostic of disease and can be used to support or deny a hypothesis. Manual measurements have the potential to be precise, but they are labor-intensive and prone to inaccuracy due to human factors (1). More and more information is being generated by CT and MR scans. The need for trustworthy automated solutions to assist radiologists in clinical diagnosis and treatment planning has consequently increased. Expert assistance has been extensively investigated in recent years, and is employed in fields like medical picture segmentation. One instance occurs labelling of voxels to identify the location of target structures in an image. Medical imaging data is made available through annual competition challenges (1). In latest ages, DL techniques like CNN become the norm for segmenting medical pictures. Fully convolutional networks and universal network (U Net) are two methods that are most frequently used in scientific studies (2, 3). Applications include multiple organ segmentation of abdominal tomographic and MRI imaging and anatomical segmentation of cardiac CT scans (4).

However, there are challenges in the generalizability of deep CNN approaches, notwithstanding their success. First, when it comes to training deep CNN models, a lot of data is better. Possible issues include the high cost of acquisition, the need for data anonymization, and patient confidentiality concerns in the biomedical imaging. Second, even though graphical processing units (GPU) usage, training volumetric medical imaging data is a time-consuming operation that necessitates a lot of resources. As a result, not only

(Received 25th February 2025; Accepted 25th June 2025; Published 25th July 2025)

performance but also computational burden should be considered for each new proposal. An essential organ, the renal excretes and filters waste products to maintain a healthy fluid and solute balance in the body. Not only does it help regulate blood pressure, but it also secretes a plethora of hormones. Figure 1 depicts the human renal (5).

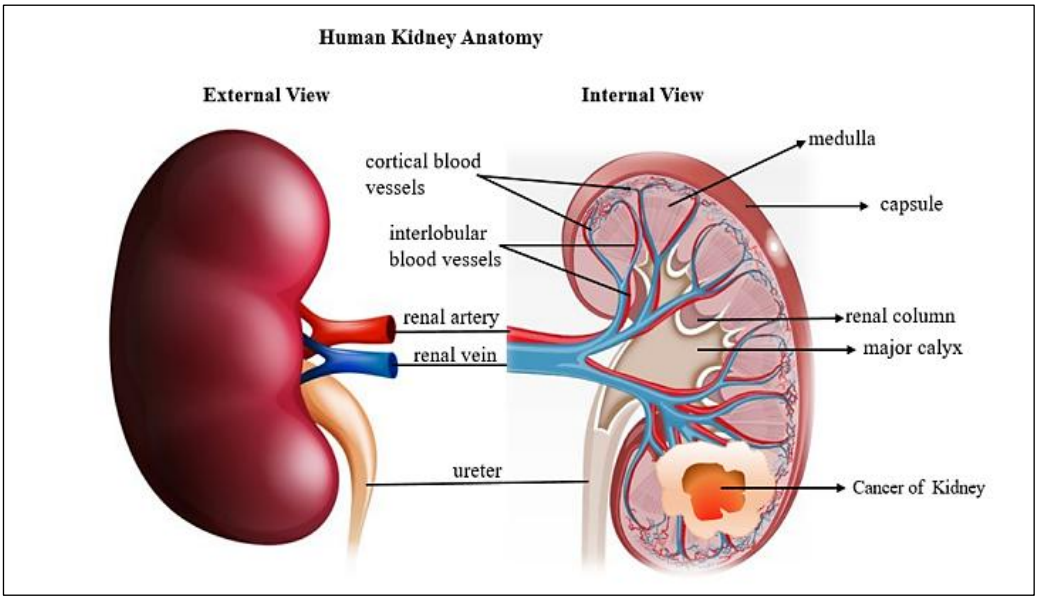

Figure 1: Renal Cell Carcinoma Developing Inside the Renal

When it comes to both sexes, renal tumor is consistently ranked high among the most common forms of the disease. About 1 in 75 people will acquire renal tumor during their lives (1.34 percent). More than 400,000 people per year are diagnosed with renal tumor (RC), an aggressive form of urological tumor (6). More than 175,000 people lose their lives to this disease each year, as reported by the Global Tumor Observatory (GCO) (7). Renal cell carcinoma (RCC) is the third highest occurrence tumor worldwide. It is anticipated that 48,780 new instances of RCC are identified annually in the United States, with 27,300 fatalities owing to the illness (8). In terms of male tumor prevalence, RCC ranks seventh and in terms of female tumor prevalence, RCC ranks ninth. It might be problematic to tell non-cancerous renal tumors from renal carcinoma on a radiograph. However, renal tumors are typically malignant. Most of these tumors are forms of Renal Cell Carcinoma (RCC) (9). According to recent data, around 80-90% of Renal malignancies are clear cell RCC (10). Since the 1990s, the global incidence rate has been rising at a pace of 2% per year.

Methodology

Deep Learning Modules for Precision Tumor Segmentation

The variability in tumor size, location, and morphological structure only adds to the difficulty of detecting malignant tissue in an abdominal organ. The liver and pancreas were segmented to a dice score of 95.43 and 79.30, respectively demonstrating that it is possible to achieve very high-quality results when Region of Interest (ROI) is the goal (11). When tumor identification is prioritized over other considerations, however, these numbers decline to 61.82 for liver tumors and 52.12 for pancreatic tumors. Likewise, there is considerable inter-organ variation in tumor classification; for instance, renal tumor detection dice scores of 93.1 and 80.2 (12).

Contrarily, the organs of the abdomen are uniform in size, shape, and location. The model might then focus on the desired organ with the help of an attentional mechanism included into the structure of the network. We used a modified version of the concept of attention gates (AG) to accomplish the ROI (13). Instead of having to physically crop the

area of interest out of the image, attention gates can find the most important parts of the picture and then selectively remove (or at least down-weight) the responses from those areas that aren't necessary for the task at hand. By incorporating Criss Cross Network (CCNet) care component, accomplishes advanced performance, with mIoU scores of 80.4 and 45.02 on the Cityscapes trial series and the ADE20K authentication group, correspondingly (14). With the use of a deep CNN model and attention modules for slice-based predictions, we were able to predict hemorrhages in 3D CT scans with human-level accuracy (15). The supervised attention mechanism empowered DAB-CNN can automatically segregate the prostate, rectum, and penile bulb (16).

Deep Learning based CT Renal Tumor Segmentation

Image processing is widely used in fields such as automation, biometrics, security monitoring, healthcare imaging, and many more. The usefulness and efficiency of an image processing task are greatly affected by the characteristic of assessment image (17). Biomedical visualization comprises ultrasound (US), computed tomography (CT), and magnetic resonance imaging (MRI). In medical imaging (MI), excellent homogeneity might obscure important details like organ borders and make it hard to identify patterns of interest. Radiologists prefer CT imaging because of the excellent quality images it produces of the body's architecture. Additionally, it provides sharp, high-contrast images. Because of this, CT imaging is crucial for the diagnosis of any renal-related illness. KiTS19 was selected to compile CT scans for 210 patients; 190 were used for training and the remaining 20 for testing. All images were downsampled to 16 × 256 × 256 voxels and their pixel levels were standardized to values between 0 and 1. Before using the AI model, expert radiologists manually labeled the kidneys and tumors, making sure all labeling remained of high clinical quality. Clinicians regularly use it to segment renal tumors for the sake of therapeutic planning (18). Furthermore, certain CT findings can be used to categorize non-malignant tumors as in Figure 2 such that the kidneys are depicted in red, and the tumor site is depicted in green.

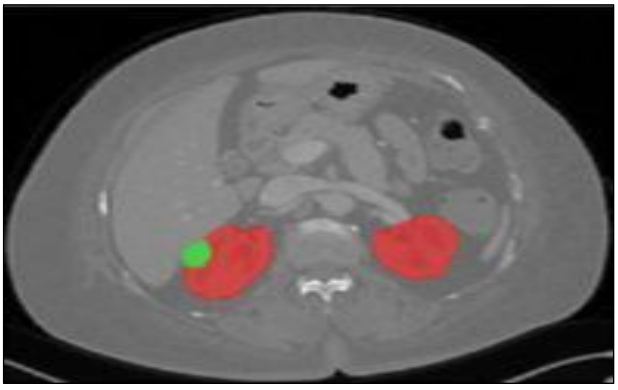

Figure 2: Images from Kits19 Data Collection Exhibiting an Axial Section across Patients' 3D CT Scans

Preliminary through initial signal, separately subsequent film x_j is computed with the help of equations as follows.

$$X_j = PW_JX_J - 1 \quad [1]$$

Summation of preceding layer's convolution is expressed in the equation as follows,

$$X_j\,(u,k_j) = \rho\,(\Sigma_k\,(X_j\text{-}1(.,K) * W_j, K_j\,(.,K))\,(u)) \quad [2]$$

$$(f*g)\,(x) = \Sigma_u = \text{-}\infty f(u)g(x\text{-}u) \quad [3]$$

Delineating tumors manually is the standard practice. The scanned medical photos of the patient will be analyzed by a radiologist with competence in segmenting any damaged parts. There is a great deal of disagreement amongst individual assessments (19). The CT technology usage retains the ability to greatly enhance disease detection and patient monitoring, leading to

improved patient care and easier assessment of therapy efficacy.

DL, a rapidly expanding subfield of machine learning, has shown promise in this application. Using deep learning techniques has been found to significantly reduce the mental load associated with visual processing (20). Semantic segmentation employs three major types of deep learning techniques: region-based, FCN, and semi-supervised. The pipeline approach is used by region-based approaches Free-form region extraction, region-based categorization, and pixel-level labeling are all implemented. To avoid the difficulty of extracting the region suggestion, FCN-based methods avoid doing so in favour of a simpler approach. The ability to map pixels individually opens up a world of possibilities for their artwork. The time required to annotate the masks can be prohibitive, and semi-supervised systems, such as semantic algorithms, often rely on a huge number of pictures. Thus, semi-supervised approaches have been introduced that make use of the annotation procedure. It has been proposed to use other DL techniques for semantic segmentation, such as feature encoders, recurrent neural networks, improved feature-based approaches, spatiotemporal feature-based methods, convolutional feature-based methods, and upsampling are all examples. The loss operation is obtained as follows,

$$\text{Loss } t = \Sigma \text{ Loss } i^{w}j \quad [4]$$

Dice factor is done with the help of equations as follows,

$$CE = \Sigma\text{-}(\text{Classes } W_c Y_{true} LOG(Y_{pred})) \quad [5]$$

$$\text{Dice\_num} = 2\ |U_{pred} \frown U_{true}| \quad [6]$$

$$\text{Dice\_den} = |U_{true}| + |U_{pred}| \quad [7]$$

$$\text{Dice} = \text{Dice\_num} / \text{Dice\_den} \quad [8]$$

Contrast–Augmented Based CT Renal Tumor Segmentation

Voxel-wise region delineation in CT and MRI data is called as 3D semantic segmentation. It covers numerous potential functions in medicine, including radiation treatment targeting, patient-specific surgical simulation, disease prognosis assessment (21, 22). A practical implementation of these applications is quite improbable, however, unless the upstream segmentation process is automated. Due to this, studies involving automatic semantic segmentation of biomedical images have proliferated. Historically, instance or semantic segmentation have been at the centre of 70% of biological big challenges (23). More memory is needed for model training and inference, and the cost of annotating data increases dramatically per instance when dealing with the third spatial dimension. Since this problem is much harder to understand than its 2D counterpart, it is difficult to harness ageing transfer learning from large, trusted computer vision standards such as ImageNet or MSCOCO. These challenges notwithstanding, recent research has shown encouraging outcomes in 3D separation of functional characteristics range and illnesses in slice imaging (24). 3D segmentation has followed the trend of using DL based algorithms in computer vision for some time now (25). The deep neural network (DNN) design space consists of many potential combinations of network architectures, optimization techniques, and training methods. As a result of DL's proven success, numerous researchers are examining this design space to see how they may improve performance. Most papers proposing a novel DNN architecture at MICCAI each year only provide results on private datasets because to the high computational cost of training DNNs, hence their results are not thoroughly benchmarked (26). The U-Net method was first proposed in early days of deep learning (DL) applications in medical picture segmentation, and later extended to 3D (27, 28). Over the years, various enhancements to U-Net have been proposed, including residual connections, dense connections, and attention approaches (29). However, showed advanced variety of trusted 3D separation main tasks utilizing simply U-Net and innovative approach to examine preprocessing operations (30). Using this guiding principle, nnU-Net recently triumphed

great challenges, in which contestants were entrusted with developing a system that excelled at the mission of ten individual magnificent trials instantaneously.

Hybrid V-Net Based Model of CT Renal Tumor Segmentation

A method for renal segmentation proposed that reduces the amount of manual processes and parameter modifications while maintaining separation precision across an extensive diversity of DCE-MRI statistics. The authors claim that after applying a five-step correction technique, their model achieves a 95% accuracy rate in segmentation, making it superior to competing algorithms (31). A technique demonstrated for robotic renal cortex separation, which allows for the completely autonomous identification of renal and cortical tissues from CT scans (32). After testing the technique on a set of 56 CTs, we stayed satisfied with its reliability. Experimental results for renal segmentation were 97.86% 2.41%, and those for renal cortex segmentation were 97.48% 3.18%.

Renal Cell Carcinoma is the utmost common type of renal tumor, and a method have just developed a decision support system to aid in its early diagnosis (33). According to their findings, death was commonly the result of renal cell tumor due to its rapid progression and the difficulty in making an early diagnosis. They used 130 datasets collected from Frat University to conduct their research, and their suggested machine learning-based decision support system successfully distinguished between normal and tumorous renal cells by 89.3%. Fully Convolutional Neural Network (FCNN) model automates renal and renal tumor segmentation (34). The need of properly segmenting renal tissues and tumors on CT scans for surgical planning was highlighted, and it was noted that renal tumor is among the ten most common types of tumors. To be more explicit, our model merges a 3D PPM with an incrementally larger feature module to create FCN that is truly novel GEFM. The suggested network design is complete learning framework based on 3D pictures, through the objective of refining tumor lesion and renal separation.

Successful segmentation of the intended structures was demonstrated in studies involving 140 patients. Renals, on average, had a Dice coefficient of 0.931, while renal tumors averaged 0.802. An approach for fragmenting renal by irregular forms was offered (35). Despite its usefulness, separation is rarely exhausted in the therapeutic discipline. These examiners are concerned in nephroblastoma affected renal, and they have suggested new CNN assessment following distinct instructing sets for physical separation. The CNN was taught valid sparse segmentation using an Over Learning Vector. The overall Dice coefficient for the study was 89.7 percent. 2D U-Net model built from CT scan data has the maximum Dice score (0.867) and hence accomplished the data test by performing cortical segmentation on kidney images using advanced U-Net versions (36). Labeling effort for training deep networks is required, but they emphasized that the approach would be more accurate if performed in 3D, by determining the capacity of renal cortex. From CT scan data, system has the maximum dice result (0.867) and hence achieved data test by performing cortical segmentation on renal images using advanced U-Net prototypes. Labeling effort for training deep networks is required, but they emphasized that the approach would be more accurate if performed in 3D, by measuring the volume of the renal cortex.

Recent work on segmenting renal cysts using CT scans described a unique hybrid segmentation strategy to CT images that allowed for improved diagnosis of renal cysts (37). The study's segmentation methodologies started with the assumption that a good prepropagation algorithm is necessary for renal segmentation in CT scans. The renal segmentation success rate was 92.12% using color-based k-means clustering techniques, and the cyst segmentation success rate was 91.24%. A U-Net centered standard for prostate separation was created due to the challenges of accurate prostate tumor identification using MRI.

A new CNN named USE-Net was created by expanding upon U-Net by inserting Squeeze-and-Excitation (SE) blocks subsequently Encoder (Enc USE-Net) or Encoder-Decoder block (Enc–Dec USE-Net). A sequence utility is used to construct SE

blocks (38). To gauge its efficacy, this model was contrasted to industry standard U-Net standard. In comparison to the early Enc U-Net and U-Net standards, the Enc-Dec U-Net standard fared better and had a higher dice constant. Though its contributions to the system in terms of running speed should be further investigated, the efficacy of SE blocks at some phases remains debatable. Nonetheless, the lessons learned from this built model can help guide the creation of future designs.

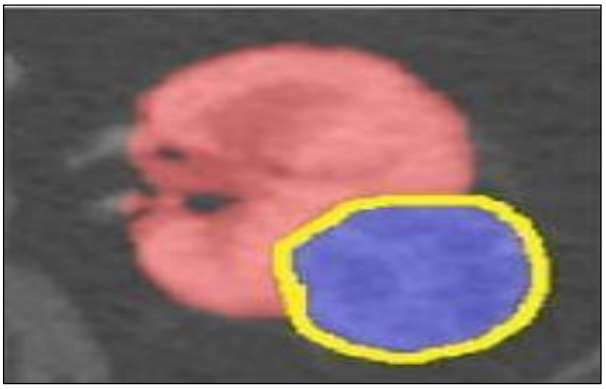

Figure 3: Renal Image Prepared by Manual Segmentation (39)

Despite these drawbacks, we nonetheless decided to use the KiTS19 dataset because to its relative rarity in the literature. The imaging data, renal and tumor borders, and existing patient characteristics were all created using a manual segmentation technique. The manual segmentation sample dataset is displayed in Figure 3.

Each CT image was downscaled to 16 × 256 × 256, besides the pixel rate was normalized from 0 to 1 by dividing by 255. There was no transfer learning applied, and the model parameters were set at random. From the resampled volumes, 64×128×128 pixel patches were selected at random for use in the training process. In total, there were 210 patients included in the dataset, with 190 serving as training data. The remaining 20 were put through various tests. The sequence of these actions was completely haphazard. Adam optimizer consumed for training, and realizing coefficient 0.001 was applied. A total of one hundred thousand epochs were chosen as the batch size. An NVIDIA Tesla V100 (32 GB, NV Link) GPU was used for the training of this model, which took roughly five days (GPU). We used the tools available in the Tensor Flow library. Figure 4 depicts a 3D level representation of the separated zones alongside while Figure 5 illustrates 2D images of a healthy renal and a renal with tumor. During this stage, the CT image is processed in order to extract useful data, such as slice texture, window thickness, and location. Both renal and tumor inside of it are unharmed. Moreover, unique photographs and masks of these areas are made.

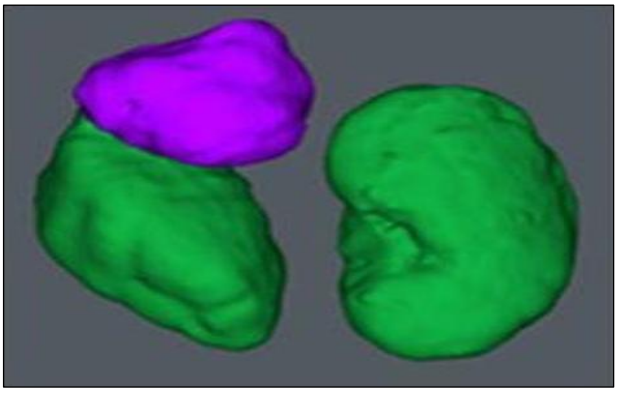

Figure 4: The Segmented Portions Are Shown in 3D Volume

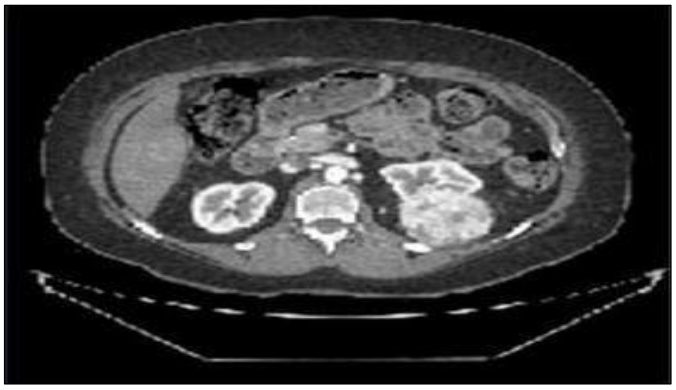

Figure 5: Picture of a Renal and Renal Cell Carcinoma (RCC) in Two Dimensions (39)

The model for segmentation applied 3D U-Net which includes an encoder-decoder structure and skip connections to maintain spatial data. Encoder blocks applied 3D convolutions, batch normalization and ReLU activation, whereas decoder blocks contained transposed convolutions. The model used the Adam optimizer (learning rate: 0.001) along with a combined Dice-cross-entropy loss to solve the class imbalance problem. The data was downsampled to 16 × 256 × 256 and then 64 × 128 × 128 patches were selected randomly. The model was trained for 100,000 epochs using the TensorFlow framework on an NVIDIA Tesla V100 (32 GB) GPU. At the beginning, weights were selected at random and no transfer learning was involved.

KiTS19 ground truth annotations were made by expert radiologists which helped ensure accuracy in clinical use. Although manual segmentation takes a lot of effort, it is considered the most accurate way. Training and validation were done with these annotations which helped the model stay reliable. Unlike full automation, some datasets such as Cityscapes and ADE20K can have semi-automated annotations that might show inconsistency.

Urography and X-rays were once the gold standards for determining a patient's renal size. Several issues were revealed in the findings acquired utilizing these techniques. Imaging techniques such as Ultrasound Sonography (US), Computed Tomography (CT), and Magnetic Resonance Imaging (MRI) can be utilized to assess renal dimension and operation. This is the first technique of its kind in the United States. They used CT and MRI to get the 3D information. Depending on the intended outcome of treatment, different diagnostic imaging techniques can be employed (40). Ultrasound (US) can be used for a wide variety of diagnostic purposes, including the detection of cysts, stones, and tumors, the provision of vital structural data without revealing patient to radioactivity, and the facilitation of a minimal expense, on-the-spot assessment. However, most of the photographs on US are subpar. This defect makes the segmentation process more troublesome than it should be. However, computed tomography (CT) is a method that provides superior images and detects even the smallest of tumors and cysts. However, being exposed to ionizing radiation is not without its risks. The prior method (magnetic resonance imaging) was insufficient. In general, MRI is an advantageous because it offers high spatial resolution with low patient risk. Its higher price is a drawback. Table 1 provides an overview of commonly used evaluation metrics for segmentation tasks.

Table 1: Segmentation Evaluation Metrics

Metric	Equation	Description
True Positive rate (TPR)	TPR = Sensitivity = Recall = ((TP) / (TP + NF))	Sensitivity measures how well a test can pick up on actual successes, or genuine positives (41).

True Negative rate (TNR)	TPR = Sensitivity = Recall = ((TP) / (TP + NF))	Specificity measures how often a test actually yields a negative result, or the true negative rate. Is it possible for a healthy person to be given a negative result by the test? This finding substantiates the test's ability to detect the lack of disease (41).
False-positive rate (FP)	FP = ((FP) / (FP + TN))	One way to quantify how often results are incorrectly marked as positive is by looking at the false-positive rate (42).
Jaccard Index (JI)	JI = ı($S_m \curvearrowright S_a$) / ($S_m + S_a$)	When comparing the statistical similarity of computationally segmented regions to those segmented by hand, the Jaccard Index (JI) was utilised (43).
Accuracy	Accuracy = ((TP + TN) / (TP + FP + NF + TN))	The accuracy of a prediction model is measured by the percentage of right predictions it makes across all completed appropriate forecasts (44).
Precision	Precision = (T_P / ($T_P + F_P$))	The positive predictive value (or accuracy) is calculated by dividing actual amount of positive scores in predicted amount of positive scores from categorization method (45).

Results and Discussion

Tissue contrast settings were changed to make the tumor more visible. Images were trimmed to highlight the abdomen and changed to 16 × 256 × 256 voxels by normalizing pixel values between 0 and 1. Dataset variability and the risk of overfitting were addressed by using data augmentation like rotation, elastic deformation and flipping, increasing the robustness of the model.

Table 2: Research Results from Research Involving Tumor Detection

Methodology	#Data	Methods	Results
Construct a DL/ML model for identifying Renal tumors	28CT	ASNN, FCM, Gabor filter	Not specified
Create a DL-based survival prediction model for people with RCC	169CT	DAG-SVM, CNN, InceptionV3	92%
Create a DL model for detecting Renal tumours	300CT	Modified CNN, 3 cross folds	91–99%

Table 2 shows studies that investigate using deep learning and machine learning with CT for detecting renal tumors. A study using ASNN, FCM and Gabor filters on 28 CT images did not disclose any performance measures. A different model predicted the survival outcomes for patients with renal cell carcinoma by using DAG-SVM, CNN and InceptionV3 and achieved 92% accuracy from 169 CT scans. The modified CNN in a third study achieved accuracy of between 99% and 91% when used on 300 CT images for finding tumors.

Table 3: Segmentation Results of Several Algorithms or Methods

Algorithms or methods	Renal Dice	Tumor Dice	Composite score
U-Net	0.482	0.444	0.463
ResU-Net	0.688	0.694	0.691
AttU-Net	0.789	0.735	0.763
R2U-Net	0.681	0.711	0.696
R2AttU-Net	0.917	0.854	0.886
nnU-Net	0.905	0.864	0.882
AlexNet+ U-Net	0.9303	\	0.9303
Hybrid V-Net	0.977	0.865	0.921
Cascaded U-Net ensembles	0.973	0.825	0.899
Cascaded volumetric convolutional network	0.974	0.831	0.902
multi-resolution VB-nets	0.973	0.832	0.903
Cascaded semantic segmentation	0.967	0.845	0.906
3d U-net based on five-fold cross-validation	0.974	0.851	0.912

Table 3 shows the segmentation accuracy scores (Dice coefficients) for kidney and tumor segmentation tasks, achieved by various algorithms. The results showed that basic U-Net models performed poorly (around 44%–48% Dice), but AttU-Net and R2AttU-Net variants led to much better accuracy (over 88%) when tested together. Hybrid and cascaded models, including Hybrid V-Net and cascaded U-Net ensembles, scored the highest with accuracy values of more than 0.90 which is the best performance for renal tumor segmentation. More generally, segmentation results are improved when complex designs and multiple approaches are used. Kidney tumors are hard to segment on CT scans because they can look very similar to the tissues around them. While performing very accurately (95% Dice scores are typical with U-Net), the accuracy decreases for small and fuzzy tumors. Challenges involve the technical difficulties related to 3D segmentation, the need for advanced computing and problems with model generalization. Attempts are being made to improve both precision and the clinical usefulness of AI models by using attention mechanisms, hybrid models and optimized training strategies.

Segmenting renal tumors with deep learning can be difficult due to variation in tumors and identifying tumors from the nearby tissues. Attention mechanisms help segmentation become more precise and this leads to high performance for U-Net and its variants (Dice scores higher than 90%). Advanced models (for instance, 3D U-Net and Hybrid V-Net) boost precision but are limited by high complexity and the value of input data. Despite the obstacles, deep learning is promising, since techniques such as semi-supervised and federated learning make large-scale, working systems in healthcare possible.

Models based on deep learning are highly accurate in tumor segmentation (reaching 95.43 Dice score) but still have issues when used in hospitals due to issues with performance variation, high computational requirements and quality of images seen in real clinical settings. The accuracy of segmenting small tumors is not as high and the model's use is limited to only one medical institution. Using methods such as federated and semi-supervised learning increases the use of AI in medical practice.

Conclusion

Modern techniques for segmenting renal and renal tumors are explored, including deep learning and building blocks. The current methods not only accurately segments, but also make up for a dearth of training data. For Renal tumors, DL can do adequate segmentation given sufficient training data. Many underperforming segmentation algorithms can be traced back to the dearth of enormous medical instructing dataset. Segmenting Renal and renal tumors has been simplified overall,

laying the groundwork for further development. Numerous contributors confirmed its status as substantial and difficult standard for 3D segmentation. Nevertheless, as test set was built from people in identical geographic area and healthcare technique as well as official unit, expanding purpose of these technologies beyond tested population is desirable. When using CT alone, the diagnostic algorithm's accuracy can be improved by including data from complementary imaging modalities like MRI or CEUS. It is recommended that researchers in DL designs, and more specifically medical imaging, steer clear of intricate architectures in any future studies. To create additional effective, general-purpose models, it is crucial to reduce the complexity of the systems to which they may be applied. The revised 2D-CNN models perform in the tumor detection and classification job, with the goals of enhancing the precision of medical diagnoses, relieving doctors and radiologists of unnecessary effort, and saving lives. In addition, the models' outputs can help lessen the possibility of incorrect diagnoses. Improved healthcare and earlier diagnosis can alter the course of disease and prolong a patient's life. Further diagnostic research, such as tumor staging and segmentation can be conducted in both renal, and further refine our technology for accurate identification and extraction of renal tumors from CT scans in the future. We hope that this new information will help us develop a reliable benchmark for the intelligent diagnosis of renal tumors.

Abbreviations

2D: Two-dimensional, 3D: Three-dimensional, ASNN: Attention-based Siamese Neural Network, CCNet: Criss-Cross Network, CEUS: Contrast-Enhanced Ultrasound, CNN: Convolutional Neural Network, CT: Computed Tomography, CT scans: Computed Tomography scans, DAB-CNN: Dual Attention Block Convolutional Neural Network, DAG-SVM: Directed Acyclic Graph Support Vector Machine, DCE-MRI: Dynamic Contrast Enhanced-Magnetic Resonance Imaging, DL: Deep Learning, DNN: Deep Neural Network, FCM: Fuzzy C-Means, FCN: Fully Convolutional Network, FP: False Positive Rate, GCO: Global Tumor Observatory, GEFM: Geodesic Entropy Functional Minimization, GPU: Graphical Processing Unit, JI: Jaccard Index, KiTS19: Kidney Tumor Segmentation 2019, MI: Medical Imaging, MICCAI: Medical Image Computing and Computer-Assisted Intervention, ML: Machine Learning, MRI: Magnetic Resonance Imaging, MR scans: Magnetic Resonance Imaging scans, MSCOCO: Microsoft Common Objects in Context, PPM: Pyramid Pooling Module, US: Ultrasound, RCC: Renal Cell Carcinoma, ROI: Region of Interest, RT: Renal Tumor, TNR: True Negative Rate, TPR: True Positive Rate, U-Net: Universal Network, V-Net: Volumetric Image Segmentation.

Acknowledgement

We acknowledge the support and encouragement from our families and friends throughout the research and writing process. Their patience and understanding have been instrumental in the completion of this paper.

Author Contributions

All authors contributed equally.

Conflict of Interest

The authors declare no conflict of interest.

Ethics Approval

The review adheres to ethical guidelines for academic research, ensuring that all sources of information are properly credited and that the integrity of the original research is maintained.

Funding

None.

References

1. Jimenez-Del-Toro O, Muller H, Krenn M, et al. Cloud-based evaluation of anatomical structure segmentation and landmark detection algorithms: VISCERAL Anatomy benchmarks. IEEE Trans Med Imaging. 2016;35:2459–75.
2. Li F, Long Z, He P, et al. Fully convolutional pyramidal networks for semantic segmentation. IEEE Access. 2020;8:229132–40.
3. Ronneberger O, Fischer P, Brox T. U-Net: Convolutional Networks for Biomedical Image Segmentation. Lecture Notes in Computer Science, Cham: Springer International Publishing. 2015:234–41. https://link.springer.com/chapter/10.1007/978-3-319-24574-4_28
4. Tran ST, Nguyen MH, Dang HP, Nguyen TT. Automatic

polyp segmentation using modified recurrent residual unet network. IEEE Access. 2022;10:65951–61.
5. Kaur R, Juneja M. A Survey of Renal Segmentation Techniques in CT Images. Curr Med Imaging Rev. 2017;14:238–50.
6. Alnazer I, Bourdon P, Urruty T, *et al.* Recent advances in medical image processing for the evaluation of chronic kidney disease. Med Image Anal 2021;69:101960.
7. Pedersen M, Andersen MB, Christiansen H, Azawi NH. Classification of renal tumour using convolutional neural networks to detect oncocytoma. Eur J Radiol. 2020;133:109343.
8. Zhang Y, Hua X, Shi H, Zhang L, Xiao H, Liang C. Systematic analyses of the role of prognostic and immunological EIF3A, a reader protein, in clear cell renal cell carcinoma. Cancer Cell Int. 2021;21:1-18.
9. Zhao W, Jiang D, Peña Queralta J, Westerlund T. MSS U-Net: 3D segmentation of kidneys and tumors from CT images with a multi-scale supervised U-Net. Inform Med Unlocked. 2020;19:100357.
10. Pan X, Quan J, Li Z, et al. miR-566 functions as an oncogene and a potential biomarker for prognosis in renal cell carcinoma. Biomed Pharmacother. 2018;102:718–27.
11. Isensee F, Petersen J, Klein A, *et al.* Abstract: nnU-net: Self-adapting framework for U-net-based medical image segmentation. Informatik aktuell, Wiesbaden: Springer Fachmedien Wiesbaden. 2019:22–22. https://arxiv.org/abs/1809.10486
12. Da Cruz LB, Araújo JDL, Ferreira JL, *et al.* Kidney segmentation from computed tomography images using deep neural network. Comput Biol Med. 2020;123:103906.
13. Kundu S, Karale V, Ghorai G, Sarkar G, Ghosh S, Dhara AK. Nested U-net for segmentation of red lesions in retinal fundus images and sub-image classification for removal of false positives. J Digit Imaging. 2022;35:1111–9.
14. Huang Z, Wang X, Wei Y, *et al.* CCNet: Criss-cross attention for semantic segmentation. IEEE Trans Pattern Anal Mach Intell. 2023;45:6896–908.
15. Gulshan V, Peng L, Coram M, Stumpe MC, Wu D, Narayanaswamy A, Venugopalan S, Widner K, Madams T, Cuadros J, Kim R. Development and validation of a deep learning algorithm for detection of diabetic retinopathy in retinal fundus photographs. jama. 2016 Dec 13;316(22):2402-10.
16. Kearney V, Chan JW, Wang T, Perry A, Yom SS, Solberg TD. Attention-enabled 3D boosted convolutional neural networks for semantic CT segmentation using deep supervision. Phys Med Biol. 2019;64:135001.
17. Goyal B, Agrawal S, Sohi BS. Noise issues prevailing in various types of medical images. Biomedical & Pharmacology Journal. 2018;11(3):1227.
18. Mu G, Lin Z, Han M, Yao G, Gao Y. Segmentation of kidney tumor by multi-resolution VB-nets. Kidney Tumor Segmentation Challenge: KiTS19. 2019 Oct;10(548719.003). https://kits.lib.umn.edu/wp-content/uploads/2019/11/gr_6e.pdf
19. Magadza T, Viriri S. Deep learning for brain tumor segmentation: a survey of state-of-the-art. Journal of Imaging. 2021 Jan 29;7(2):19.
20. Guo Y, Liu Y, Georgiou T, Lew MS. Analysis of Semantic Segmentation Using Deep Neural Networks. Int J Multimed Inf Retr. 2018;7:87–93.
21. He T, Hu J, Song Y, Guo J, Yi Z. Multi-task learning for the segmentation of organs at risk with label dependence. Med Image Anal. 2020;61:101666.
22. Blake P, Sathianathen N, Heller N, Rosenberg J, Rengel Z, Moore K. Automatic renal nephrometry scoring using machine learning. European Urology Supplements. 2019;18:e904-905.
23. Maier-Hein L, Eisenmann M, Reinke A, Onogur S, Stankovic M, Scholz P, Arbel T, Bogunovic H, Bradley AP, Carass A, Feldmann C. Why rankings of biomedical image analysis competitions should be interpreted with care. Nature communications. 2018 Dec 6;9(1):5217.
24. Zhuang X, Li L, Payer C, *et al.* Evaluation of algorithms for Multi-Modality Whole Heart Segmentation: An open-access grand challenge. Med Image Anal. 2019;58:101537.
25. Litjens G, Kooi T, Bejnordi BE, Setio A, Ciompi F, Ghafoorian M. A survey on deep learning in medical image analysis. Med Image Anal. 2017;42:60–88.
26. Heller N, Rickman J, Weight C, Papanikolopoulos N. The role of publicly available data in MICCAI papers from 2014 to 2018. Lecture Notes in Computer Science, Cham: Springer International Publishing; 2019:70–7. https://www.researchgate.net/publication/335257994_The_Role_of_Publicly_Available_Data_in_MICCAI_Papers_from_2014_to_2018
27. Zhang D, Zhou H, Zhou T, Chang Y, Wang L, Sheng M, Jia H, Yang X. Using 2D U-Net convolutional neural networks for automatic acetabular and proximal femur segmentation of hip MRI images and morphological quantification: a preliminary study in DDH. BioMedical Engineering OnLine. 2024 Oct 5;23(1):98.
28. Çiçek Ö, Abdulkadir A, Lienkamp SS, Brox T, Ronneberger O. 3D U-net: Learning dense volumetric segmentation from sparse annotation. Medical Image Computing and Computer-Assisted Intervention – MICCAI 2016, Cham: Springer International Publishing. 2016:424–32. https://www.researchgate.net/publication/304226155_3D_U-Net_Learning_Dense_Volumetric_Segmentation_from_Sparse_Annotation
29. Alzubaidi L, Zhang J, Humaidi AJ, *et al.* Review of deep learning: concepts, CNN architectures, challenges, applications, future directions. J Big Data. 2021;8:53.
30. Fayyaz AM, Sharif MI, Azam S, Karim A, El-Den J. Analysis of Diabetic Retinopathy (DR) based on the deep learning. Information (Basel). 2023;14:30.
31. Xin Y, Minh HL, Cheng KT, Sung KH, Liu W. Renal Compartment segmentation in DCE-MRI images. Med Image Anal. 2016;32:269–80.
32. Baghdadi A, Aldhaam NA, Elsayed AS, *et al.* Automated differentiation of benign renal oncocytoma and

chromophobe renal cell carcinoma on computed tomography using deep learning: AI-assisted differentiation of oncocytoma vs chromophope tumours. BJU Int. 2020;125:553–60.
33. Iqbal M, Shah MD, Vun-Sang S, Okazaki Y, Okada S. The therapeutic potential of curcumin in alleviating N-diethylnitrosamine and iron nitrilotriacetate induced renal cell tumours in mice via inhibition of oxidative stress: Implications for cancer chemoprevention. Biomed Pharmacother. 2021;139:111636.
34. Badrinarayanan V, Kendall A, Cipolla R. SegNet: A deep convolutional encoder-decoder architecture for image segmentation. IEEE Trans Pattern Anal Mach Intell. 2017;39:2481–95.
35. Rhalem I, Bouanani Z, Akammar A, *et al.* Using imaging to diagnose renal tumors beyond nephroblastoma. Radiol Case Rep. 2024;19:2773–80.
36. Couteaux V, Si-Mohamed S, Renard-Penna R, *et al.* Kidney cortex segmentation in 2D CT with U-Nets ensemble aggregation. Diagn Interv Imaging. 2019;100:211–7.
37. Moldovanu CG. Virtual and augmented reality systems and three-dimensional printing of the renal model-novel trends to guide preoperative planning for renal cancer. Asian J Urol. 2024;11:521–9.
38. Rundo L, Han C, Nagano Y, *et al.* USE-Net: Incorporating Squeeze-and-Excitation blocks into U-Net for prostate zonal segmentation of multi-institutional MRI datasets. Neurocomputing. 2019;365:31–43.
39. Türk F, Lüy M, Barışçı N. Kidney and renal tumor segmentation using a hybrid V-Net-based model. Mathematics. 2020;8:1772.
40. Torres HR, Queirós S, Morais P, Oliveira B, Fonseca JC, Vilaça JL. Kidney segmentation in ultrasound, magnetic resonance and computed tomography images: A systematic review. Comput Methods Programs Biomed. 2018;157:49–67.
41. Aljabri M, AlGhamdi M. A review on the use of deep learning for medical images segmentation. Neurocomputing. 2022;506:311–35.
42. Kaur R, Juneja M, Mandal AK. A hybrid edge-based technique for segmentation of renal lesions in CT images. Multimed Tools Appl. 2019;78:12917–37.
43. Abdelrahman A, Viriri S. Kidney tumor semantic segmentation using deep learning: A survey of state-of-the-art. J Imaging. 2022;8:55.
44. Wu H, Yang S, Huang Z, He J, Wang X. Type 2 diabetes mellitus prediction model based on data mining. Inform Med Unlocked. 2018;10:100–7.
45. Saito T, Rehmsmeier M. The precision-recall plot is more informative than the ROC plot when evaluating binary classifiers on imbalanced datasets. PLoS One. 2015;10:e0118432.